Polymer 50 (2009) 397–403

Contents lists available at ScienceDirect

Polymer

journal homepage: www.elsevier.com/locate/polymer

Synthesis, electron mobility, and electroluminescence of a polynorbornene-supported silole

Xiaowei Zhan [a,b,*], Andreas Haldi [c], Junsheng Yu [c], Takeshi Kondo [c], Benoit Domercq [c], Jian-Yang Cho [a], Stephen Barlow [a], Bernard Kippelen [c,**], Seth R. Marder [a,***]

[a] School of Chemistry and Biochemistry and Center for Organic Photonics and Electronics, Georgia Institute of Technology, Atlanta, GA 30332, USA
[b] Beijing National Laboratory for Molecular Sciences and CAS Key Laboratory of Organic Solids, Institute of Chemistry, Chinese Academy of Sciences, Beijing 100190, China
[c] School of Electrical and Computer Engineering and Center for Organic Photonics and Electronics, Georgia Institute of Technology, Atlanta, GA 30332, USA

ARTICLE INFO

Article history:
Received 9 September 2008
Received in revised form
20 November 2008
Accepted 21 November 2008
Available online 30 November 2008

Keywords:
Polynorbornene-supported silole
Electron mobility
Light-emitting diodes

ABSTRACT

A solution-processable polynorbornene with pendant fluorescent and electron-transport silole groups was synthesized using ruthenium-complex-initiated ring-opening metathesis polymerization. A weight-average molecular weight around 59,300 and a low polydispersity index of 1.4 were estimated for the polymer using gel permeation chromatography. The thermal, electronic, photo- and electroluminescence properties of the polymer were investigated and compared with those of a small-molecule reference compound. The polymer exhibits better thermal stability than the small molecule and exhibits a glass transition temperature of 91 °C, while retaining the optical and electronic properties of the corresponding small-molecule silole. The room temperature electron mobility was measured using the time-of-flight technique to be 3.5×10^{-5} $cm^2/V/s$ at an applied electric field of 7.5×10^5 V/cm. Organic light-emitting diodes fabricated using the polymer as the electron transport and emissive layer have low efficiencies; introduction of an additional tris(8-hydroxyquinolinato)aluminum (Alq_3) electron-transport layer leads not only to increased efficiency, but also to increased contributions to the electroluminescence from the Alq_3.

1. Introduction

Recent studies on siloles (silacyclopentadienes) suggest that these systems could be useful in organic electronic applications. Relatively high electron mobilities have been measured for siloles and, in some cases, the mobilities have been found to be unaffected by exposure to air [1]. The electron affinities of several 1,1-diaryl-2,3,4,5-tetraphenylsiloles were recently measured using inverse-photoemission spectroscopy (IPES) and were found to be comparable to that of the well-established electron-transport (ET) material tris(8-hydroxyquinolinato)aluminum (Alq_3) [2], suggesting comparable ease of electron injection in the silole and Alq_3 systems. Siloles possess photoluminescence (PL) quantum yields that are among the highest reported for neat organic films [3]. Capitalizing on these properties, some groups have used siloles as materials for electrogenerated chemiluminescence [4], in chemo- and biosensors for detecting chemical (e.g., explosives) [5] and biological analytes (e.g., antibodies) [6], and in various electronic devices such as light-emitting diodes (OLEDs) [7], solar cells [8], and field-effect transistors (OFETs) [9].

One limitation associated with many small-molecule siloles is their poor solution processability [7]. Since current trends in device fabrication favor solution processing, we have begun to explore the utility of high molecular-weight side-chain silole polymers as an approach to the fabrication of large-area thin-film devices by spin-coating or ink-jet printing. Several research groups have worked on the preparation of polymers containing siloles in the main or side chains [10]. For synthesis of the polymers with siloles in the main chain, most of the methods are based on polycondensation reactions. A number of homopolymers of silole [11], dibenzosilole [12], dithienosilole [13], and fused silole [14], as well as copolymers with fluorene [15], thiophene [16], diethynylbenzene [17], silicon [18], carbazole [19], and triphenylamine [20], have been synthesized. Another approach to silole polymers is to attach siloles to side chains of the polymers. Only a few papers reported this kind of silole polymers; polyacetylene [21], polyethylene [22], and poly(methacrylate) [23] have been used as main chains to support pendant siloles.

* Corresponding author. Beijing National Laboratory for Molecular Sciences and CAS Key Laboratory of Organic Solids, Institute of Chemistry, Chinese Academy of Sciences, 2 Bei-Yi Street, Beijing 100190, China. Tel.: +86 10 62533098; fax: +86 10 62559373.
** Corresponding author.
*** Corresponding author.
E-mail addresses: xwzhan@iccas.ac.cn (X. Zhan), kippelen@ece.gatech.edu (B. Kippelen), seth.marder@chemistry.gatech.edu (S.R. Marder).

0032-3861/$ – see front matter © 2008 Elsevier Ltd. All rights reserved.
doi:10.1016/j.polymer.2008.11.035

Ring-opening metathesis polymerization (ROMP) initiated by ruthenium alkylidene complexes has proven to be an excellent method for the preparation of polymers that is compatible with many functional groups [24]. Furthermore, ROMP is often a living polymerization method, offering the possibility of polymers with controlled molecular weights and low polydispersities, and also allowing for the formation of block copolymers [25]. In this work, we report the synthesis of a monomer in which a fluorescent silole is covalently bound to norbornene and the homopolymerization of this monomer. We compare the polymer, **2**, with a small-molecule reference silole, **1** (Fig. 1). The electronic and optical properties of the polymer in solution are found similar to those of the small molecule analogue in solid state. Finally, solution-processed OLED devices based on the polymer are fabricated and characterized.

2. Experimental section

2.1. Materials

Diphenylacetylene, trichlorophenylsilane, lithium wire, and magnesium shavings were purchased from Aldrich and used as-received without further purification. 5-(5-Bromopentyl)-norbornene was prepared according to published procedures [26]. The 3rd generation Grubbs initiator was synthesized from the 1st generation initiator (Strem) according to the literature procedure [27].

2.2. Characterization

The ^{1}H and ^{13}C NMR spectra were measured on a Varian Mercury 300 spectrometer using tetramethylsilane ($\delta = 0$ ppm) as an internal standard. High-resolution mass spectra (HRMS) were measured on a VG Instruments 70-SE using the electron impact (EI) mode. Elemental analyses were carried out by Atlantic Microlabs using a LECO 932 CHNS elemental analyzer. Solution (chloroform) and thin-film (on quartz substrate) UV–vis absorption spectra were recorded on a Varian Cary 5E UV–vis–NIR spectrophotometer, while solution (chloroform) and thin-film PL spectra were recorded on a Shimadzu FP-5301PC spectrofluorometer. Electrochemical measurements were carried out under nitrogen on a deoxygenated solution of tetra-*n*-butylammonium hexafluorophosphate (0.1 M) in acetonitrile using a computer-controlled BAS 100B electrochemical analyzer, a glassy-carbon working electrode, a platinum-wire auxiliary electrode, and a Ag wire anodized with AgCl as a pseudo-reference electrode. Potentials were referenced to the ferrocenium/ferrocene ($FeCp_2^{+/0}$) couple by using ferrocene as an internal standard. Thermogravimetric analysis (TGA) was carried out using a Shimadzu thermogravimetric analyzer (model TGA-50) under a nitrogen flow at a heating rate of 10 °C/min. Differential scanning calorimeter (DSC) was carried out using Shimadzu differential scanning calorimeter (model DSC-50) under a nitrogen flow at a heating rate of 10 °C/min and a cooling rate of 20 °C/min. Gel permeation chromatography (GPC) analyses were carried out using a Shimadzu instrument coupled to a multidiode array UV detector with tetrahydrofuran (THF) as an eluent on American Polymer Standards 10 μm particle size, linear mixed bed packing columns. All GPCs were calibrated using polystyrene standards.

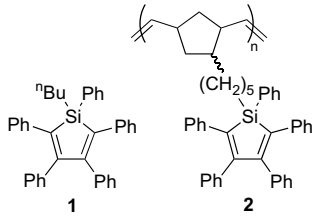

Fig. 1. Structures of a reference small-molecule silole, **1**, and norbornene silole polymer **2**.

2.3. Time-of-flight mobility measurement

The electron mobility of the polymer was characterized using the time-of-flight (TOF) technique. The polymer was heated above the glass transition temperature between two indium tin oxide (ITO) electrodes and a 20 μm-thick film was fabricated using calibrated glass spacers. Samples were then sealed with epoxy. An electric field was applied to the sample and a photocurrent was generated with a 6-ns pulse of a nitrogen laser (337 nm). The generated photocurrent was amplified with a low-noise preamplifier and the transient signal was monitored on a digital oscilloscope.

2.4. Preparation of electroluminescence devices

The photo-crosslinkable bis(diarylamino)biphenyl-based polymer **3** [28] (Fig. 2) and the silole polymer **2** were used as hole-transport layer and emissive layer, respectively. Furthermore, an electron-transport layer of Alq_3 was evaporated on some devices. The configuration of the device was ITO/**3** (35 nm)/**2** (40 nm)/Alq_3 (*x* nm)/LiF (1 nm)/Al where *x* was 0, 10, or 35 nm. A 35 nm-thick hole-transport layer was spin-coated from 10 mg/mL toluene solution of **3** onto air-plasma-treated ITO-coated glass substrates with a sheet resistance of 20 Ω/square (Colorado Concept Coatings, L.L.C). The film was crosslinked using a standard broad band UV light with a 0.7 mW/cm^2 power density for 1 min. Subsequently, a 40 nm-thick emissive layer was spin-coated from a 10 mg/mL chloroform solution of **2** onto the crosslinked hole-transport layer. For the electron-transport layer, Alq_3 was first purified using gradient zone sublimation, and films were then thermally evaporated at a rate of 1 Å/s and at a pressure below 1×10^{-7} torr on top of the emissive layer. 1 nm of lithium fluoride (LiF) and a 200 nm-thick aluminum cathode were deposited in vacuum at a pressure below 1×10^{-6} torr and at rates of 0.1 Å/s and 2 Å/s, respectively. A shadow mask was used for the evaporation of the top metal electrode to form five devices per substrate with an area of 0.1 cm^2 each. At no point during fabrication were the devices exposed to atmospheric conditions. The testing was done immediately after the deposition of the metal cathode in inert atmosphere without exposing the devices to air.

2.5. Synthesis

2.5.1. 1-Chloro-1,2,3,4,5-pentaphenylsilole (*I*)

This intermediate was prepared according to a procedure reported by Chen et al. [29]. Diphenylacetylene (16.8 mmol, 3.0 g) and clean lithium shavings (14 mmol, 98 mg) were put in a 100 mL

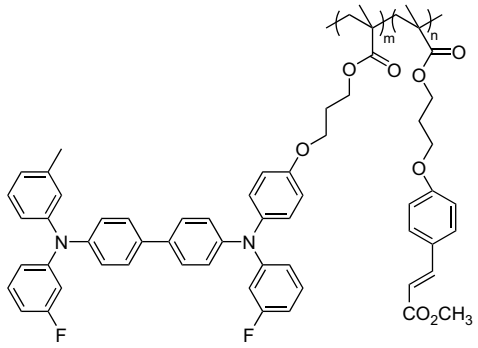

Fig. 2. Chemical structure of polymer **3**.

three-necked round bottom flask and deoxygenated with nitrogen for 30 min. 15 mL of dry THF was then added. The reaction mixture was stirred at room temperature for 14 h under nitrogen atmosphere. The resultant deep green mixture was diluted with 30 mL of dry THF, and added dropwise to a solution of trichlorophenylsilane (6.3 mmol, 1.33 g) in 20 mL of dry THF over a period of 0.5 h at room temperature. The brown mixture was stirred at the same temperature for 2 h, and then refluxed for 5 h to give a dark yellow solution. The THF solution of the resultant reactive intermediate **I** was used in situ for the synthesis of siloles without isolation.

*2.5.2. 1-Butyl-1,2,3,4,5-pentaphenylsilole (**1**) [30]*

4.0 mL of 1.6 M *n*-BuLi (6.4 mmol) in hexane was dropwise added to the THF solution of **I** at −78 °C over a period of 10 min. The mixture was stirred at the same temperature for 1 h and was gradually warmed to room temperature; the solution was stirred overnight. The resulting yellow-green solution was washed with water; the organic layer was extracted with diethyl ether and dried over anhydrous $MgSO_4$. The solvent was removed and the residue was purified by flash column chromatography over silica gel using hexane/dichloromethane = 8/1 as eluent. Recrystallization from ethanol gave faintly greenish-yellow and highly blue fluorescent crystals (2.74 g, 84%, based on trichlorophenylsilane). Mp (DSC): 156 °C. ^{1}H NMR (300 MHz, $CDCl_3$): δ 7.64 (m, 2H), 7.36 (m, 3H), 7.03 (m, 12H), 6.86 (m, 8H), 1.51 (m, 2H), 1.39 (m, 4H), 0.85 (t, J = 7.2 Hz, 3H). ^{13}C NMR (75 MHz, $CDCl_3$): δ 155.99, 139.66, 139.48, 138.82, 134.79, 132.98, 129.84, 129.69, 128.88, 128.06, 127.67, 127.33, 126.16, 125.39, 26.18, 25.50, 13.86, 10.56. HRMS (EI), calcd for $C_{38}H_{34}Si$ (M^+): 518.2430. Found: 518.2438. Anal. Calcd for $C_{38}H_{34}Si$: C, 87.98; H, 6.61. Found: C, 87.69; H, 6.63%. UV ($CHCl_3$), λ_{max} (ε_{max}) 251 (2.79×10^4), 365 (1.10×10^4) nm ($mol^{-1}\,L\,cm^{-1}$).

*2.5.3. 1-(5-Norbornenyl-pentyl)-1,2,3,4,5-pentaphenylsilole (**II**)*

To a 250 mL three-necked round bottom flask were added magnesium shavings (10 mmol, 240 mg), 5-(5-bromopentyl)-norbornene (approximately 95% pure endo isomer, 6.3 mmol, 1.53 g) and a little iodine and deoxygenated with nitrogen for 30 min. 20 mL of dry THF was added, and the mixture was stirred at 40 °C for 8 h. The color of the mixture was changed from light red to colorless then to light gray. The gray Grignard reagent suspension was cooled to 0 °C, and transferred portionwise into the THF solution of **I** over a period of 30 min. The deep greenish brown mixture was stirred for 1 h at 0 °C, was gradually warmed to room temperature, and was stirred overnight. The resulting yellow-green solution was washed with water; the organic layer was extracted with diethyl ether, and dried over $MgSO_4$. The solvent was removed and the residue was purified by flash column chromatography over silica gel using hexane/dichloromethane = 8/1 as eluent and recrystallization from methanol to afford a pale yellow solid with strong blue fluorescence (1.26 g, 32%, based on 5-(5-bromopentyl)-norbornene). Mp (DSC): 109 °C. ^{1}H NMR (300 MHz, $CDCl_3$): δ 7.64 (m, 2H), 7.34 (m, 3H), 7.01 (m, 12H), 6.85 (m, 8H), 6.08 (m, 1.3H), 5.87 (m, 0.7H), 2.72 (s, 2H), 1.93–1.76 (m, 2H), 1.53 (m, 2H), 1.42–1.16 (m, 8H), 1.00 (m, 2H), 0.46 (m, 1H). ^{13}C NMR (75 MHz, $CDCl_3$): δ 155.98, 139.75, 139.48, 138.85, 136.70, 134.79, 133.01, 132.31, 129.85, 129.69, 128.90, 128.08, 127.68, 127.35, 126.18, 125.42, 49.57, 45.43, 42.56, 38.75, 34.67, 33.26, 32.50, 28.28, 23.36, 10.82. HRMS (EI), calcd for $C_{46}H_{44}Si$ (M^+): 624.3212. Found: 624.3182. Anal. Calcd for $C_{46}H_{44}Si$: C, 88.41; H, 7.10. Found: C, 88.28; H, 7.15%. UV ($CHCl_3$), λ_{max} (ε_{max}) 250 (2.26×10^4), 365 (0.89×10^4) nm ($mol^{-1}\,L\,cm^{-1}$).

*2.5.4. Poly[1-(5-norbornenyl-pentyl)-1,2,3,4,5-pentaphenylsilole] (**2**)*

The silole monomer **II** (0.5 mmol, 312 mg) was dissolved in 5 mL of chloroform. 5 mL of chloroform solution of the 3rd generation Grubbs initiator (5 μmol, 4.42 mg) was added to the monomer solution and stirred for 30 min, followed by the addition of ethyl vinyl ether (1 mL). After stirring for an additional 10 min, the solution was concentrated down to 5 mL and added dropwise to 100 mL of ethanol. The polymer, which precipitated out of solution, was collected and redissolved in 5 mL of chloroform and reprecipitated into ethanol. The final product was collected as a pale yellow fiber-like solid (300 mg, 96%). ^{1}H NMR (300 MHz, $CDCl_3$): δ 7.60 (m, 2H), 7.30 (m, 3H), 6.96–6.83 (m, 20H), 5.20 (br, 2H), 2.90–2.30 (br, 2H), 1.82 (br, 3H), 1.50–0.80 (br, 10H). ^{13}C NMR (75 MHz, $CDCl_3$): δ 155.92, 139.75, 139.43, 138.78, 134.73, 132.93, 129.81, 129.67, 128.84, 128.06, 127.68, 127.35, 126.16, 125.42, 45.44, 43.18, 42.47, 40.06, 37.10, 33.33, 31.72, 28.26, 23.42, 10.76. Anal. Calcd for $(C_{46}H_{44}Si)_n$: C, 88.41; H, 7.10. Found: C, 88.01; H, 7.12%. UV ($CHCl_3$), λ_{max} (ε_{max}) 250 (2.55×10^4), 365 (0.98×10^4) nm ($mol^{-1}\,L\,cm^{-1}$).

3. Results and discussion

3.1. Synthesis and characterization of the polymer

The synthesis of the silole-containing norbornene monomer **II** and homopolymer **2** is shown in Scheme 1. The known intermediate 1-chloro-1,2,3,4,5-pentaphenylsilole (**I**) was prepared according to a published procedure [29] from the ring-closing reaction of 1,4-dilithio-1,2,3,4-tetraphenyl-1,3-butadiene with trichlorophenylsilane. The known reference compound 1-*n*-butyl-1,2,3,4,5-pentaphenylsilole (**1**), which has previously been obtained from 1,2,3,4,5-pentaphenylsilole [30], was prepared from the reaction of intermediate **I** with *n*-butyllithium shown in Scheme 1.

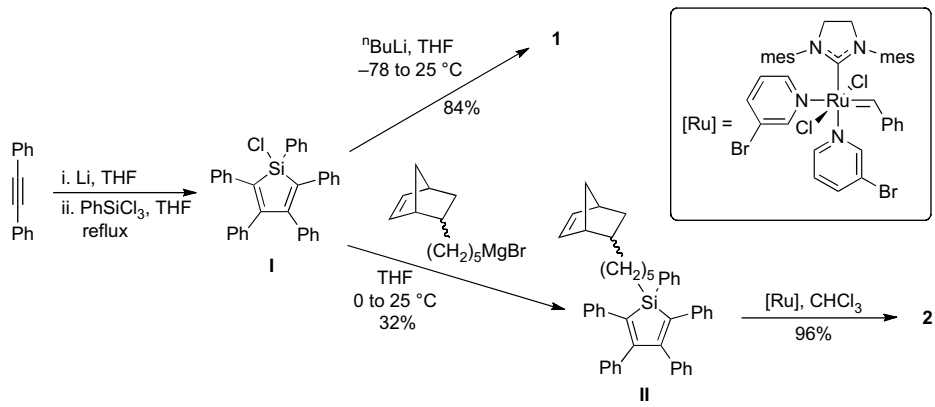

Scheme 1. Synthetic routes of **1** and **2** (mes = 2,4,6-trimethylphenyl).

The new silole-containing norbornene monomer **II** was prepared from the reaction of the intermediate **I** with the Grignard reagent derived from 5-(5-bromopentyl)norbornene. The polymerization was carried out using the 3rd generation Grubbs' ruthenium initiator in chloroform at room temperature to afford the polymer **2** in high yield.

The polymerization was monitored by ^{1}H NMR spectroscopy and was deemed complete when no signals attributable to norbornene ring olefinic protons were detected. The weight-average molecular weight (M_w) and polydispersity index of the polymer were estimated to be 59,300 and 1.4, respectively, using GPC (polystyrene standards). The degree of polymerization of the polymer was estimated to be *ca* 68, while the target degree of polymerization was 100, i.e., monomer to catalyst ratio of 100:1 was employed. Thermogravimetric analysis studies demonstrate that the onset weight-loss temperature (T_{TGA}) of the polymer **2** is 415 °C, much higher than that (313 °C) for the small molecule **1** (Fig. 3). The DSC curves of **1** and **2** are illustrated in Fig. 3. When the crystalline sample of the reference **1** was heated, an endothermic peak due to melting was observed at 156 °C, but no glass transition was observed even on the 2nd heating. While the polymer sample of **2** was heated, a glass transition was observed at 91 °C, but no melting point, suggesting that the polymer is amorphous, which is advantageous for OLEDs.

3.2. Electronic and optical properties

Cyclic voltammograms of reference compound **1** show two features assignable to molecular oxidation peaks and two to molecular reduction, while the polymer **2** shows one oxidation peak and one reduction peak (Fig. 4), none of which appears fully reversible, indicating the charged species to be unstable in solution. The peak potentials corresponding to the first oxidation and the first reduction for **1** and **2** are similar: the anodic peak potentials (E_{pa}) vs $FeCp_2^{+/0}$ of **1** and **2** are +0.94 and +1.02 V respectively, while the cathodic peak potentials (E_{pc}) vs $FeCp_2^{+/0}$ of **1** and **2** are −2.30 and −2.37 V respectively.

Solution and thin-film UV–vis absorption spectra for **1** and **2** are shown in Fig. 5. The absorption spectrum of the polymer **2** shows identical peaks (365 nm in solution and 369 nm in film) as that of the reference **1**, indicating that incorporation of the silole into a polymer does not significantly affect its electronic structure. Absorption in the solid state for **1** and **2** is similar to that in solution with only modest red shifts, as seen for other siloles [2].

Solution and thin-film PL spectra of **1** and **2** are shown in Fig. 5. The polymer **2** and the reference **1** show weak greenish blue luminescence in solution, with very similar emission spectra peaked at 484 nm, demonstrating that the emission properties of the silole are retained in the polymer. Consistent with other siloles [31], the fluorescence appears to be considerably stronger in the solid state

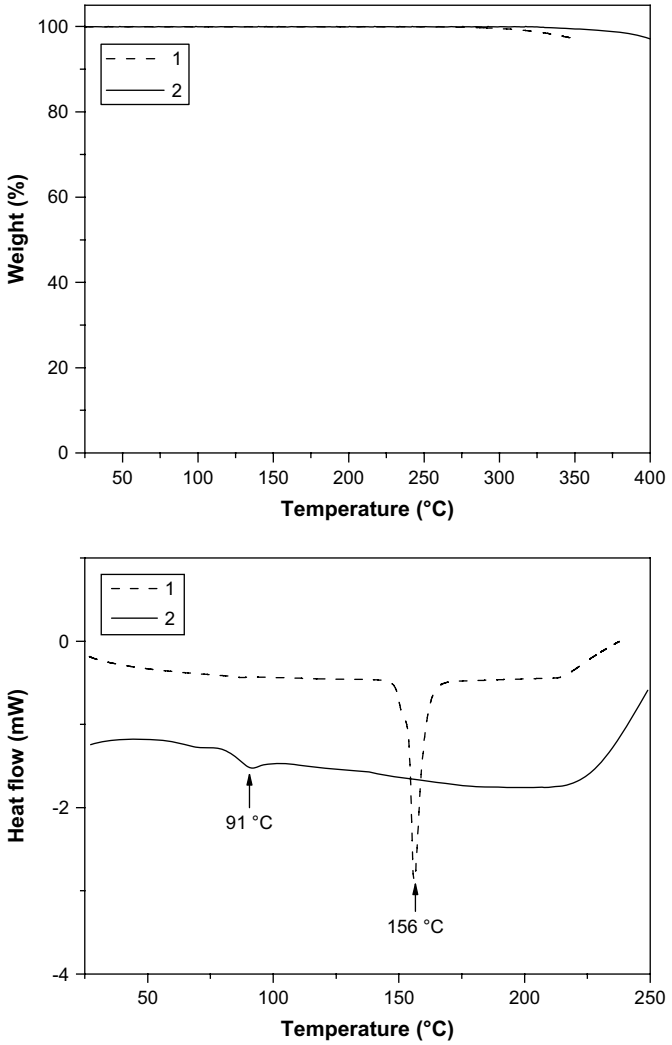

Fig. 3. TGA (top) and DSC (bottom) curves of **1** and **2**.

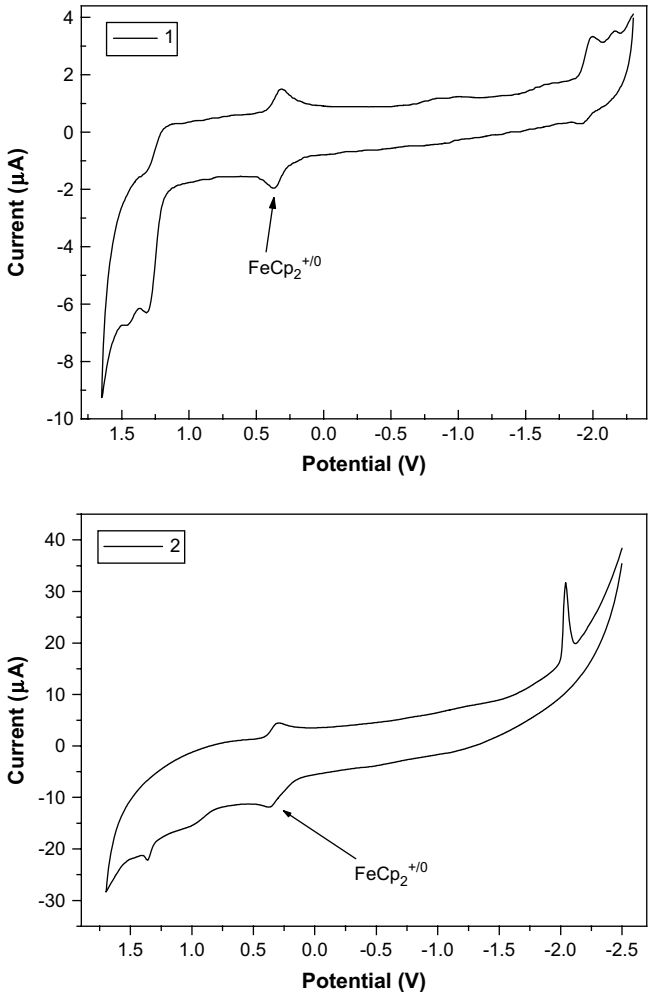

Fig. 4. Cyclic voltammograms of **1** and **2** (with $FeCp_2$ as an internal reference) in CH_3CN/0.1 M $[^nBu_4N]^+[PF_6]^-$ at 50 mV/s. The horizontal scale refers to an anodized Ag wire pseudo-reference electrode.

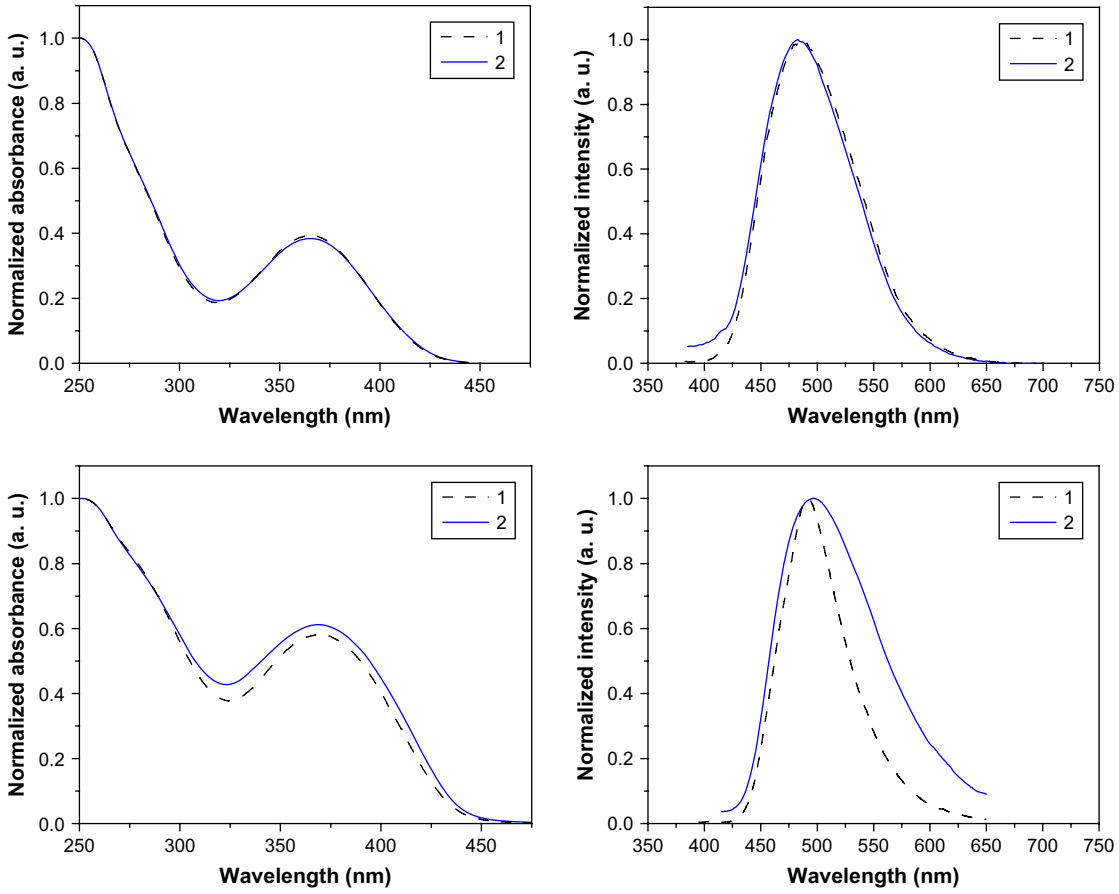

Fig. 5. Solution (chloroform) [top left] and thin-film [bottom left] UV–vis absorption spectra and solution (chloroform) [top right] and thin-film [bottom right] fluorescence spectra of **1** and **2**.

relative to that in solution with the maxima at slightly lower energies. The feature seen in the solid state band for **1** is narrower relative to that in solution, while PL spectrum in the solid state for **2** is broader than that in solution, for reasons unclear at present.

Electrochemistry, electronic absorption, and fluorescence studies clearly show that the electronic and optical properties of the silole **1** are largely preserved in the polymer **2** and not affected by the polymer backbone.

3.3. Electron mobility and electroluminescence

The electron mobility of the polymer was measured using the time-of-flight (TOF) technique. Fig. 6 shows typical generated photocurrents as a function of time measured at two different values of the applied electric field at room temperature. Both of the plots exhibit a plateau, followed by a decay. The electron mobility μ was calculated from the equation $\mu = d^2/t_t V$ where d is the thickness of the sample, V is the applied voltage, and where the transit time t_t was determined from a time-of-flight transient in a double logarithmic plot as shown in the inset of Fig. 6 due to the dispersive nature of the transients. At an applied electric field of 7.5×10^5 V/cm the room temperature electron mobility was calculated to be 3.5×10^{-5} cm^2/V/s. This value is in the same range as those reported for small-molecule siloles and Alq_3 [32]. However, it is lower than the highest electron mobility reported for the bipyridine-containing silole for which a mobility of 2.0×10^{-4} cm^2/V/s was reported at an applied electric field of 6.4×10^5 V/cm [1].

The electron-transport and photoluminescence properties of the silole polymer **2** suggest that this polymer is suitable for OLEDs in a bilayer geometry in conjunction with a hole-transport material. However, as previously reported by Chen et al. [7d], the most efficient device structure identified thus far for silole-based OLEDs is multilayer devices with an emissive silole layer inserted between hole- and electron-transport layers. Therefore, for this study, similar 2- and 3-layer OLEDs based on **2** were fabricated and

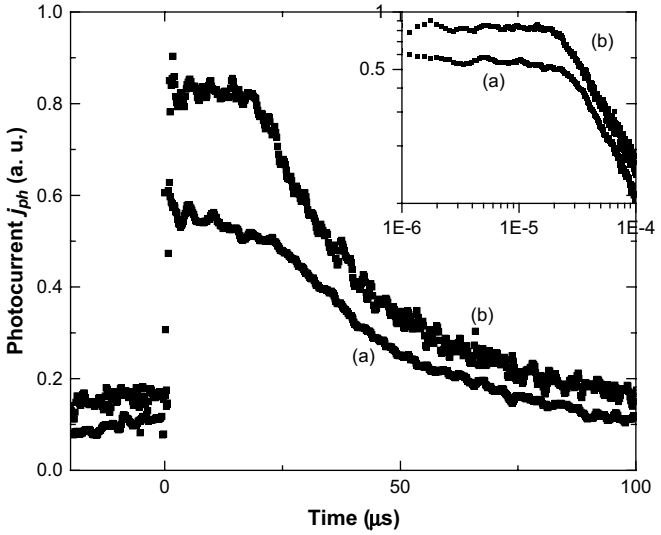

Fig. 6. Time-of-flight signal measured at two applied electric fields $E = 7.0 \times 10^5$ (a) and 7.5×10^5 V/cm (b) for a 20 μm-thick sample of **2** at room temperature. The inset shows the same data in a double logarithmic plot to determine the transient time from the intersection of linear fits to the slopes at short and at long times.

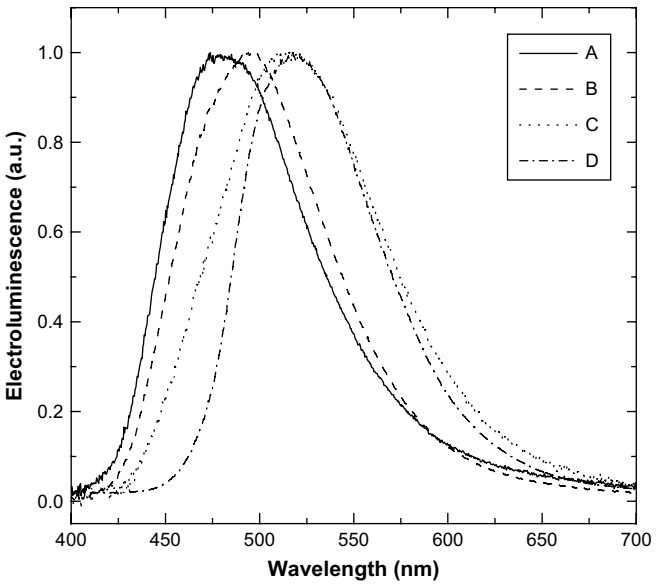

Fig. 7. Normalized electroluminescence spectra of devices with structure **A**: ITO/**3** (35 nm)/**2** (40 nm)/LiF (1 nm)/Al (solid line), structure **B**: ITO/**3** (35 nm)/**2** (40 nm)/Alq_3 (10 nm)/LiF (1 nm)/Al (dashed line), structure **C**: ITO/**3** (35 nm)/**2** (40 nm)/Alq_3 (35 nm)/LiF (1 nm)/Al (dotted line), and structure **D**: ITO/TPD (50 nm)/Alq_3 (50 nm)/LiF (1 nm)/Al (dash-dotted line).

characterized. The hole-transport layer consisted of the photo-crosslinkable TPD-based polymer **3** [28]. The silole polymer was dissolved in chloroform and spin-coated to yield 40 nm-thick films. For some devices, a thermally evaporated film of Alq_3 of 10 nm or 35 nm thickness served as the electron-transport layer. Finally, a 1 nm-thick layer of LiF was used as electron-injection layer, and a 200 nm-thick layer of aluminum acted as the cathode. Typical electroluminescence spectra measured for devices with the structure ITO/**3** (35 nm)/**2** (40 nm)/Alq_3 (*x* nm)/LiF (1 nm)/Al where *x* is 0, 10, or 35 nm are shown in Fig. 7. The electroluminescence spectrum of the device without Alq_3 was similar to the photoluminescence spectrum of **2**. However, with increasing thickness of the Alq_3 layer the electroluminescence peak showed a red shift where the devices with a 35-nm thick film exhibited an electroluminescence that originated almost explicitly from Alq_3, as indicated in Fig. 7 by a device with the structure ITO/TPD (50 nm)/Alq_3 (50 nm)/LiF (1 nm)/Al. Hence, it is possible that the observed red shift resulted from an energy transfer from **2** to Alq_3 and could therefore be avoided by using an electron-transport material with a wider bandgap.

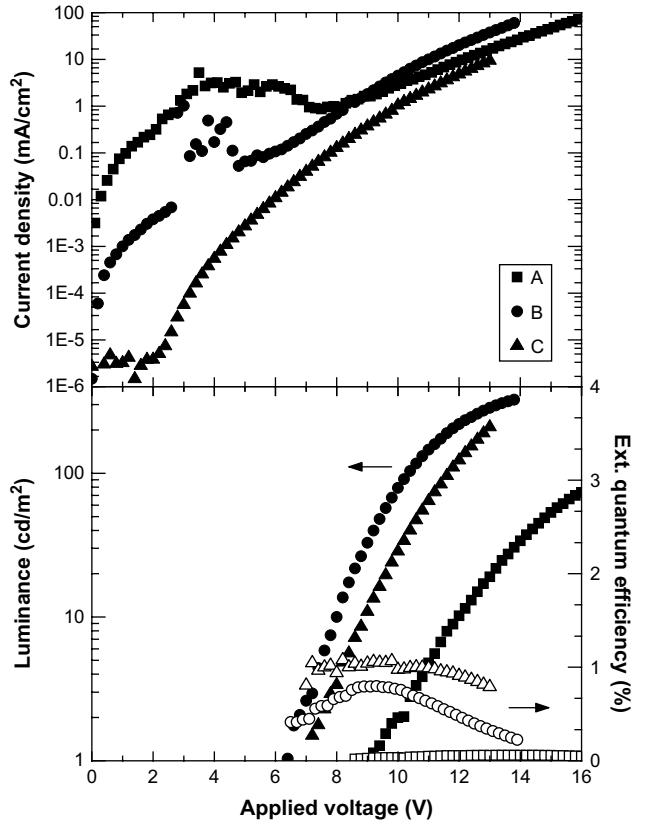

Fig. 8. Current density (above), luminance (solid symbols, below) and external quantum efficiency (empty symbols, below) as a function of applied voltage for devices with structure **A**: ITO/**3** (35 nm)/**2** (40 nm)/LiF (1 nm)/Al (squares), structure **B**: ITO/**3** (35 nm)/**2** (40 nm)/Alq_3 (10 nm)/LiF (1 nm)/Al (circles), and structure **C**: ITO/**3** (35 nm)/**2** (40 nm)/Alq_3 (35 nm)/LiF (1 nm)/Al (triangles).

The current densities, the luminances, and the external quantum efficiencies (EQE) as a function of the applied voltage for the devices with the structure ITO/**3** (35 nm)/**2** (40 nm)/Alq_3 (*x* nm)/LiF (1 nm)/Al are shown in Fig. 8. Similar to other reports of OLEDs based on polymers with silole pendants in the side chains [21b,22], very low efficiencies were observed in devices without an additional electron-transport layer. However, the efficiencies increased significantly in devices with a 10-nm or 35-nm thick layer of Alq_3 where the devices with the 35-nm thick film of Alq_3 exhibited an EQE of 0.9% at 100 cd/m^2, comparable to the efficiencies that were measured in OLEDs with the device structure ITO/**3** (60 nm)/Alq_3 (60 nm)/Mg:Ag [28]. The incorporation of **2**, therefore, obviously did not have a significant influence on the device performance. Devices with only a 10-nm thick layer of Alq_3, on the other hand, showed only slightly lower efficiencies (0.7%, 1.7 cd/A), while the contribution of the silole polymer to the emission was clearly visible. The efficiencies of these devices were comparable to the efficiencies that were reported for devices using small-molecule siloles as emissive layer in a similar 3-layer device structure as reported here [33], and they were significantly higher than the two reports of OLEDs based on polymers with silole pendants in the side chains published thus far, which reported efficiencies between 0.1% and 0.2% in a 2- or 3-layer device structure [21b,22].

4. Conclusions

We have synthesized a norbornene-based homopolymer with an electron transport and emissive silole in the side chain via ROMP. In comparison with the small-molecule reference silole, the polymer shows good solution processability, excellent thermal stability, and amorphous morphology. By comparing the silole-containing polymer to its small-molecule analogue, we established that the polymer backbones do not interfere with the basic photophysical properties of the silole. The electron mobility of the polymer is comparable to those reported for some small-molecule siloles and Alq_3. The OLED device using the polymer as the emissive layer exhibits higher efficiencies than those reported for the devices using other polymers with silole pendants as emissive layer. While the results here are not competitive with other state-of-the-art small molecule and polymer devices, they nonetheless demonstrate that solution-based fabrication of OLED devices can be fabricated from silole-functionalized poly(norbornene)s.

Acknowledgements

This material is based upon work supported in part by the National Science Foundation STC Program under Agreement Number DMR-0120967. We also thank the NSF for support through grants DMR-0408589 and DMR-0420863 and the Office of Naval

Research for support through a MURI (Award Number N00014-03-1-0793, administered through the California Institute of Technology). X.Z. thanks the Chinese Academy of Sciences for support through Hundred Talents Program.

References

[1] Murata H, Malliaras GG, Uchida M, Shen Y, Kafafi ZH. Chem Phys Lett 2001;339:161–6.
[2] Zhan X, Risko C, Amy F, Chan C, Zhao W, Barlow S, et al. J Am Chem Soc 2005;127:9021–9.
[3] Murata H, Kafafi ZH, Uchida M. Appl Phys Lett 2002;80:189–91.
[4] Sartin MM, Boydston AJ, Pagenkopf BL, Bard AJ. J Am Chem Soc 2006;128:10163–70.
[5] (a) Sohn H, Sailor MJ, Magde D, Trogler WC. J Am Chem Soc 2003;125:3821–30;
(b) Toal SJ, Jones KA, Magde D, Trogler WC. J Am Chem Soc 2005;127:11661–5;
(c) Toal SJ, Trogler WC. J Mater Chem 2006;16:2871–83.
[6] (a) Chan CPY, Haeussler M, Tang BZ, Dong YQ, Sin KK, Mak WC, et al. J Immunol Methods 2004;295:111–8;
(b) Dong YQ, Lam JWY, Qin A, Li Z, Liu J, Sun J, et al. Chem Phys Lett 2007;446:124–7.
[7] (a) Tamao K, Uchida M, Izumizawa T, Furukawa K, Yamaguchi S. J Am Chem Soc 1996;118:11974–5;
(b) Ohshita J, Nodono M, Kai H, Watanabe T, Kunai A, Komaguchi K, et al. Organometallics 1999;18:1453–9;
(c) Tang BZ, Zhan XW, Yu G, Lee PPS, Liu YQ, Zhu DB. J Mater Chem 2001;11:2974–8;
(d) Chen HY, Lam WY, Luo JD, Ho YL, Tang BZ, Zhu DB, et al. Appl Phys Lett 2002;81:574–6;
(e) Lee J, Liu QD, Bai DR, Kang Y, Tao Y, Wang S. Organometallics 2004;23:6205–13;
(f) Geramita K, McBee J, Shen YL, Radu N, Tilley TD. Chem Mater 2006;18:3261–9;
(g) Lee J, Yuan YY, Kang YJ, Jia WL, Lu ZH, Wang S. Adv Funct Mater 2006;16:681–6;
(h) Son HJ, Han WS, Chun JY, Lee CJ, Han JI, Ko J, et al. Organometallics 2007;26:519–26.
[8] (a) Mi B, Dong Y, Li Z, Lam JWY, Haeussler M, Sung HHY, et al. Chem Commun 2005:3583–5;
(b) Liao L, Dai L, Smith A, Durstock M, Lu J, Ding J, et al. Macromolecules 2007;40:9406–12;
(c) Boudreault PLT, Michaud A, Leclerc M. Macromol Rapid Commun 2007;28:2176–9;
(d) DiCarmine PM, Wang X, Pagenkopf BL, Semenikhin OA. Electrochem Commun 2008;10:229–32;
(e) Wang E, Wang L, Lan L, Luo C, Zhuang W, Peng J, et al. Appl Phys Lett 2008;92:033307.
[9] (a) Ohshita J, Lee KH, Hamamoto D, Kunugi Y, Ikadai J, Kwak YW, et al. Chem Lett 2004;33:892–3;
(b) Usta H, Lu G, Facchetti A, Marks TJ. J Am Chem Soc 2006;128:9034–5;
(c) Kim DH, Ohshita J, Lee KH, Kunugi Y, Kunai A. Organometallics 2006;25:1511–6;
(d) Lu G, Usta H, Risko C, Wang L, Facchetti A, Ratner MA, et al. J Am Chem Soc 2008;130:7670–85.
[10] Chen JW, Cao Y. Macromol Rapid Commun 2007;28:1714–42.
[11] (a) Yamaguchi S, Jin RZ, Itami Y, Goto T, Tamao K. J Am Chem Soc 1999;121:10420–1;
(b) Yamaguchi S, Jin RZ, Tamao K. J Am Chem Soc 1999;121:2937–8;
(c) Sohn H, Huddleston R, Powell DR, West R, Oka K, Xu Y. J Am Chem Soc 1999;121:2935–6.
[12] (a) Chan KL, McKiernan MJ, Towns CR, Holmes AB. J Am Chem Soc 2005;127:7662–3;
(b) Mo YQ, Tian RY, Shi W, Cao Y. Chem Commun 2005:4925–6.
[13] Ohshita J, Hamamoto D, Kimura K, Kunai A. J Organomet Chem 2005;690:3027–32.
[14] Xu C, Yamada H, Wakamiya A, Yamaguchi S, Tamao K. Macromolecules 2004;37:8978–83.
[15] (a) Liu MS, Luo J, Jen AKY. Chem Mater 2003;15:3496–500;
(b) Wang F, Luo J, Yang K, Chen J, Huang F, Cao Y. Macromolecules 2005;38:2253–60;
(c) Wang EG, Li C, Mo Y, Zhang Y, Ma G, Shi W, et al. J Mater Chem 2006;16:4133–40.
[16] (a) Tamao K, Yamaguchi S, Shiozaki M, Nakagawa Y, Ito Y. J Am Chem Soc 1992;114:5867–9;
(b) Yamaguchi S, Goto T, Tamao K. Angew Chem Int Ed 2000;39:1695–7;
(c) Lee Y, Sadki S, Tsuie B, Reynolds JR. Chem Mater 2001;13:2234–6.
[17] (a) Corriu RJP, Douglas WE, Yang ZX. J Organomet Chem 1993;456:35–9;
(b) Boydston AJ, Yin Y, Pagenkopf BL. J Am Chem Soc 2004;126:10350–4;
(c) Wong WY, Wong CK, Poon SY, Lee AWM, Mo T, Wei X. Macromol Rapid Commun 2005;26:376–80.
[18] (a) Sanji T, Sakai T, Kabuto C, Sakurai H. J Am Chem Soc 1998;120:4552–3;
(b) Adachi A, Yasuda H, Sanji T, Sakurai H, Okita K. J Lumin 2000;87–89:1174–6.
[19] Wang Y, Hou L, Yang K, Chen J, Wang F, Cao Y. Macromol Chem Phys 2005;206:2190–8.
[20] Xiao H, Leng B, Tian H. Polymer 2005;46:5707–13.
[21] (a) Chen J, Xie Z, Lam JWY, Law CCW, Tang BZ. Macromolecules 2003;36:1108–17;
(b) Chen J, Kwok HS, Tang BZ. J Polym Sci Part A Polym Chem 2006;44:2487–98.
[22] Lee KH, Ohshita J, Kimura K, Kunugi Y, Kunai A. J Organomet Chem 2005;690:333–7.
[23] Ma Z, Ijadi-Maghsoodi S, Barton TJ. Polym Prepr (Am Chem Soc Div Polym Chem) 1997;38:249.
[24] Grubbs RH. Handbook of metathesis, vol. 3. Weinheim: Wiley-VCH; 2003.
[25] Trnka TM, Grubbs RH. Acc Chem Res 2001;34:18–29.
[26] Stubbs LP, Weck M. Chem Eur J 2003;9:992–9.
[27] Love JA, Morgan JP, Trnka TM, Grubbs RH. Angew Chem Int Ed 2002;41:4035–7.
[28] Domercq B, Hreha RD, Zhang YD, Larribeau N, Haddock JN, Schultz C, et al. Chem Mater 2003;15:1491–6.
[29] Chen J, Law CCW, Lam JWY, Dong Y, Lo SMF, Williams ID, et al. Chem Mater 2003;15:1535–46.
[30] (a) Curtis MD. J Am Chem Soc 1969;91:6011–8;
(b) Jutzi P, Karl A. J Organomet Chem 1981;214:289–302.
[31] Luo J, Xie Z, Lam JWY, Cheng L, Chen H, Qiu C, et al. Chem Commun 2001:1740–1.
[32] (a) Yu G, Yin S, Liu Y, Chen J, Xu X, Sun X, et al. J Am Chem Soc 2005;127:6335–46;
(b) Barth S, Muller P, Riel H, Seidler PF, Riess W, Vestweber H, et al. J Appl Phys 2001;89:3711–9.
[33] Zhan X, Haldi A, Risko C, Chan CK, Zhao W, Timofeeva TV, et al. J Mater Chem 2008;18:3157–66.